ADVANCED MATERIALS
www.advmat.de

Kerr Nonlinearity in 2D Graphdiyne for Passive Photonic Diodes

Leiming Wu, Yuze Dong, Jinlai Zhao, Dingtao Ma, Weichun Huang, Ye Zhang, Yunzheng Wang, Xiantao Jiang, Yuanjiang Xiang, Jianqing Li, Yaqing Feng, Jialiang Xu,* and Han Zhang**

Graphdiyne is a new carbon allotrope comprising sp- and sp^2-hybridized carbon atoms arranged in a 2D layered structure. In this contribution, 2D graphdiyne is demonstrated to exhibit a strong light–matter interaction with high stability to achieve a broadband Kerr nonlinear optical response, which is useful for nonreciprocal light propagation in passive photonic diodes. Furthermore, advantage of the unique Kerr nonlinearity of 2D graphdiyne is taken and a nonreciprocal light propagation device is proposed based on the novel similarity comparison method. Graphdiyne has demonstrated a large nonlinear refractive index in the order of $\approx 10^{-5}$ cm^2 W^{-1}, comparing favorably to that of graphene. Based on the strong Kerr nonlinearity of 2D graphdiyne, a nonlinear photonic diode that breaks time-reversal symmetry is demonstrated to realize the unidirectional excitation of Kerr nonlinearity, which can be regarded as a significant demonstration of a graphdiyne-based prototypical application in nonlinear photonics and might suggest an important step toward versatile graphdiyne-based advanced passive photonics devices in the future.

Carbon-based nanomaterials such as fullerene,[1–3] carbon nanotube,[4–6] graphene,[7–9] and graphdiyne[10–12] have been discovered and attracted worldwide attention in the past a few decades, for their excellent optical, thermal, and electrical properties.[13] These carbon allotropes are made of carbon atoms with different hybrid states such as sp^3, sp^2, and sp. For instance, diamond can be formed by sp^3, while carbon nanotube and graphene can be constructed by the hybridization of sp^3 and sp^2 carbons.[8,14] Graphdiyne, a novel 2D carbon allotrope first synthesized by Li et al., is characterized by the hybridization of sp and sp^2 carbons with large area ($\approx$3.61 cm^2) and high stability.[10] Graphdiyne has excellent electrical, optical, and thermal properties to have demonstrated remarkable performances in optoelectronic devices.[11] The intrinsic mobility of graphdiyne, as calculated by Chen et al.[15] with the method of Boltzmann transport equation and the deformation potential theory, is 4.29×10^5 cm^2 V^{-1} s^{-1} for holes and 5.41×10^5 cm^2 V^{-1} s^{-1} for electrons, which is much higher than that of graphene ($\approx 3 \times 10^5$ cm^2 V^{-1} s^{-1}).[15] Graphdiyne has been also predicted to be the most stable carbon network containing diacetylenic linkages.[16,17] The bandgap of graphdiyne has been calculated to be in the range of 0.46–1.22 eV according to different calculation methods.[18–20] Graphdiyne possesses suitable bandgaps and ultrahigh carrier mobilities, and therefore has wider prospects than conventional 2D materials such as graphene, MoS_2, Bi_2Se_3, and black phosphorus for optoelectronic applications. In this context, graphdiyne has been widely applied in various research fields, such as catalysts,[21,22] batteries,[23,24] solar cells,[25,26] and sensors.[27,28] However, the applications of graphdiyne in photonics are still in its infancy. In this contribution, we experimentally measured and investigated the nonlinear optical (NLO) properties of 2D graphdiyne and further designed a novel photonic diode based on graphdiyne by using the method of spatial self-phase modulation (SSPM).

Dr. L. Wu, Dr. J. Zhao, Dr. D. Ma, Prof. J. Li
Faculty of Information Technology
Macau University of Science and Technology
Macao 519020, P. R. China
Dr. L. Wu, Dr. W. Huang, Dr. Y. Zhang, Dr. Y. Wang, Dr. X. Jiang, Prof. Y. Xiang, Prof. H. Zhang
Shenzhen Engineering Laboratory of Phosphorene and Optoelectronics
Key Laboratory of Optoelectronic Devices and Systems of Ministry of Education and Guangdong Province
College of Optoelectronic Engineering
Shenzhen University
Shenzhen 518060, P. R. China
E-mail: hzhang@szu.edu.cn
Dr. Y. Dong, Prof. Y. Feng
School of Chemical Engineering and Technology
Tianjin University
Yaguan Road 135, Tianjin 300350, P. R. China
E-mail: yqfeng@tju.edu.cn
Prof. J. Xu
School of Materials Science and Engineering
National Institute for Advanced Materials
Tianjin Key Lab for Rare Earth Materials and Applications
Nankai University
Tongyan Road 38, Tianjin 300350, P. R. China
E-mail: jialiang.xu@nankai.edu.cn
The ORCID identification number(s) for the author(s) of this article can be found under https://doi.org/10.1002/adma.201807981.

DOI: 10.1002/adma.201807981

Currently, there are three main methods for measuring the nonlinear properties of 2D materials, namely the four wave mixing, Z-scan, and SSPM measurements. Hendry et al.[29] and Zhang et al.[30] reported respectively the feasibilities of the methods of four wave mixing and Z-scan to study the nonlinear optical property of graphene and found the third-order nonlinear optical susceptibility ($\chi^{(3)}_{\text{monolayer}}$) for graphene is in the range of $\approx 10^{-7}$ e.s.u. The SSPM method, first created by Durbin et al.,[31] has been also widely used to measure the nonlinear refractive indexes of new 2D materials such as graphene,[32] MoS_2,[33] black phosphorus,[34] and Bi_2Te_3.[35] In 2011, Wu et al.[32] investigated the nonlinear optical response in chemically exfoliated graphene based on the SSPM method and found the same magnitude of third-order NLO susceptibility ($\chi^{(3)}_{\text{monolayer}} \approx 10^{-7}$ e.s.u.). By comparison, we can find that the results obtained from these three methods (four wave mixing, Z-scan and SSPM) match well. However, in the method of four wave mixing and Z-scan, the requirements of the optical path are more complicated, while the schematic diagram of SSPM is very simple.

The realization of nonreciprocal light propagation is the main purpose to design photonic diodes, which have been applied in many fields ranging from optical telecommunications to integrated photonics.[36] The conventional ways to realize the optical nonreciprocity include the interband photonic transitions,[37,38] optomechanical systems,[39,40] specially designed wave-guides,[41,42] micro-resonator systems[36,43] etc. Although 2D materials have been applied in many optical devices such as detectors,[44] switchers,[45] modulators,[46] and sensors[47] in the past decade, their application in photonic diode has been relatively unexplored. Recently, Dong et al.[48] demonstrated a passive photonic diode based on the saturable absorption behavior of 2D Ti_3C_2 MXene by using the open aperture Z-scan method, which opens the possibility of applying 2D materials in photonic diode. Herein, we have proposed a novel configuration of nonlinear photonic diode to achieve the nonreciprocal light propagation by using the SSPM method based on 2D materials represented by graphdiyne and SnS_2. It is demonstrated that graphdiyne has a narrow bandgap to support a broadband nonlinear optical response when a laser beam passes through. While SnS_2 exhibits a behavior of reverse saturable absorption (RSA)[49] with a large bandgap (2.6 eV), it is difficult to excited the diffraction rings. When the two materials are coupled together to create a hybrid graphdiyne/SnS_2 structure, the phenomenon of propagational symmetry-breaking between the forward (graphdiyne/SnS_2) and reverse (SnS_2/graphdiyne) directions occurs to realize the unidirectional diffraction rings excitation. Two ways might be used to realize the nonreciprocal light propagation in the 2D material based photonic diode, namely the nonreciprocal propagation of light transmittance and the nonreciprocal propagation of light shape. The photonic diode based on nonreciprocal propagation of light intensity has been reported by Dong et al.[48] with the Z-scan method. Herein, we have proposed another photonic diode based on nonreciprocal propagation of light shape with the method of SSPM. Our results show that the hybrid structure of graphdiyne/SnS_2 can achieve the nonreciprocal light propagation, indicating the graphdiyne 2D materials can operate as a positive role in nonlinear photonic diode.

2D graphdiyne is fabricated by the liquid/liquid interfacial synthesis method.[50] The upper liquid layer is a solution of catalyst in water for acetylenic homocoupling containing copper (II) acetate and pyridine, while the bottom liquid layer is the dichloromethane layer containing hexaethynylbenzene (HEB) monomer (**Figure 1**a). In order to circumvent a random encounter between HEB and the catalyst, a middle layer of pure water is initially overlaid between the layers. After the catalytic coupling reaction for 24 h, 2D graphdiyne is produced at the liquid/liquid interface. Figure 1b shows the atomic force microscopy (AFM) image of the fabricated 2D graphdiyne, in which the height is measured to be ≈4.1 nm. To test the optical stability of the 2D graphdiyne under the laser exposure, the graphdiyne suspension is exposed under a 532 nm laser beam for 5 h. The result shows that the transmittances of the 2D graphdiyne dispersions change very slightly after 5 h of exposure (Figure 1c), indicating the high stability of the 2D graphdiyne sample (Figure S1, Supporting Information). In addition, clear lattice fringes of ≈0.45 nm is clearly observed in the high-resolution transmission electron microscopy (TEM) image (Figure 1d), in accordance with the characteristic graphdiyne.[51] Moreover, an obvious selected area electron diffraction (SAED) pattern can also be obtained (Figure 1e), demonstrating the high crystallinity of the graphdiyne film. Finally, the size distribution of as-prepared 2D graphdiyne is shown in Figure 1f, and the average size of the graphdiyne suspension is ≈458 nm. The bandgap of the graphdiyne sample was determined to be $E_g = 0.81$ eV by the Tauc plot curve as shown in Figure 1g. The Raman spectrum of 2D graphdiyne showed its characteristics bands with peak maxima at 1378, 1575, 1920, and 2168 cm^{-1} (Figure 1h). The high-resolution X-ray photoelectron spectroscopy (XPS) can discern the chemical environment of an element, which is shown in Figure 1i. The abundance ratio of the sp/sp^2 carbons is ≈1.5, which is in good agreement with the chemical composition of graphdiyne.

Figure 2 shows the NLO response of graphdiyne suspension with the SSPM method pumped at λ = 671, 532, and 457 nm, respectively. From the obtained patterns of diffraction rings as shown in Figure 2b, it can be noticed that the incident light first expanded into a circular pattern at a short time, and then quickly collapsed into a semi-circular pattern due to the nonaxis-symmetrical thermal convection (NASTC) caused by the heat of laser beam.[53] The variation of ring numbers with respect to the intensity of laser beam as shown in Figure 2c shows that a stronger NLO response can be obtained from a relatively low wavelength. The optical bandgap of the graphdiyne was measured to be as narrow as 0.81 eV in our experiment, which means that the laser wavelengths of 457 nm (2.71 eV), 532 nm (2.33 eV) and 671 nm (1.85 eV) can be used as light sources to interact with 2D graphdiyne. The laser with wavelength of 457 nm is theoretically capable of interacting with the materials with a bandgap $E_g < 2.71$ eV. Comparing to the laser of 532 nm (2.33 eV) and 671 nm (1.85 eV), the 457 nm laser is farther away from the bandgap of 2D graphdiyne to excite more electrons from the valence band to the conduction band. Therefore, the 457 nm laser can produce a strongest nonlinear optical response in our experiment. The distortion caused by NASTC can produce an effect to the nonlinear refractive index of 2D graphdiyne. These results indicate that the change in NLO response ($\Delta n_2/n_2$) will first increase to the largest and then

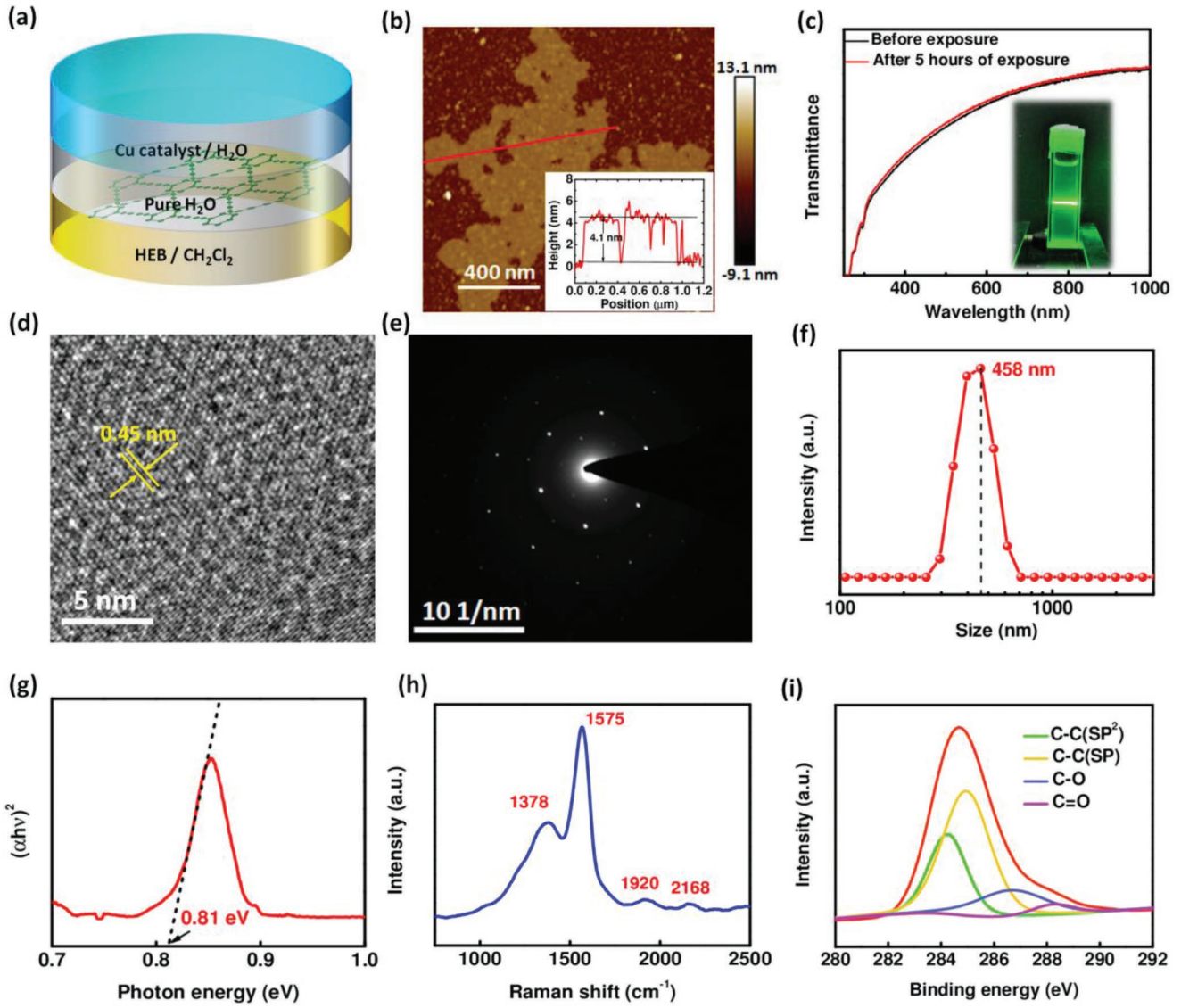

Figure 1. a) A schematic representation of the liquid/liquid interfacial synthesis. b) AFM image of the as-prepared 2D graphdiyne. The inset cross-section profile shows the height of the graphdiyne film is ≈4.1 nm. c) The optical stability of the 2D graphdiyne under the exposure of laser beam. d) The high-resolution TEM image and e) SAED pattern for the 2D graphdiyne. f) The size distribution of the as-prepared 2D graphdiyne. g) Tauc plot curve of the graphdiyne. h) Raman spectrum of graphdiyne. i) High-resolution C 1s spectra of graphdiyne.

become saturated at the process of distortion (Figure S2, Supporting Information). Here, Here, N and I are the number of diffraction rings and incident intensity. From the experimental data, we can find that the N and I show a linear relationship (Figure 2c). Hence we can obtain its slope value (dN/dI) after fitting, the value of $dN/dI \approx N/I$. The change of the nonlinear refractive index is due to nonaxis-symmetrical thermal convection of the dispersions, and the NASTC is closely related to the intensity of the laser beam. It can be found that the depth of the distortion is becoming more and more obvious due to the heat of laser beam, and the heat process is the enhancement process of nonaxis-symmetrical thermal convection. With the enhancement of the NASTC, the graphdiyne in the upper part of the dispersion will be squeezed into the lower part of the dispersion to have a smaller density to obtain a relatively low refractive index, and this will lead to a change in the number of diffraction rings, then the value of N/I will be changed, and further lead to the change in nonlinear refractive index. The nonlinear optical response of 2D graphdiyne at different concentration is shown in Figure S3 in the Supporting Information. The concentration of graphdiyne used in our experiment is 0.2 mg mL^{-1}, and the nonlinear optical response is 0.256 cm^2 W^{-1} at λ = 457 nm. When the concentration increases to 0.4 mg mL^{-1}, the nonlinear optical response of graphdiyne will show a corresponding improvement to 0.567 cm^2 W^{-1} dues to an increase in the number of graphene layers passed by the laser.

Taking advantage of the SSPM method, we proposed a novel nonlinear photonic diode which used the hybrid structure of the 2D graphdiyne/SnS_2 (**Figure 3**a) to achieve the directional excitation of the Kerr nonlinearity. The laser sources with

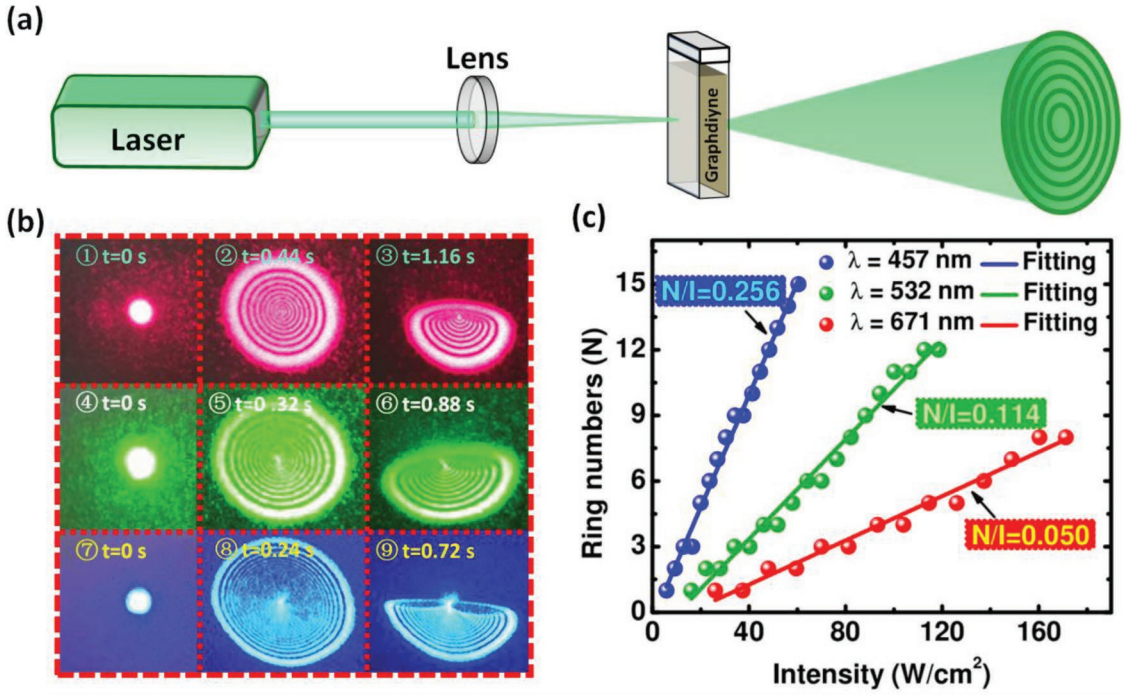

Figure 2. a) The SSPM experiment for the independent graphdiyne dispersions. b) The patterns of diffraction rings obtained at λ = 671, 532, and 457 nm. c) The NLO response for graphdiyne suspensions at different wavelengths.

wavelengths of 532 and 671 nm are used to pump the hybrid graphdiyne/SnS_2 sample. When the laser beam with a relatively high intensity passes from the forward (graphdiyne/SnS_2) direction of the nonlinear photonic diode, the diffraction rings will be excited due to the strong NLO response of graphdiyne caused by Kerr effect (Figure 3b③,⑤). However, when the laser beam with same intensity passes from the reverse (SnS_2/graphdiyne) direction, the diffraction rings cannot be produced (Figure 3b④,⑥). The reason is that the SnS_2 have strong linear absorption to severely reduce the intensity of incident light. When the laser beam (λ = 532 nm) passes through the SnS_2 dispersions (Figure 3d), the intensity of incident light will be reduced to a lower level which is below the threshold to excite the diffraction rings of graphdiyne. When an incident 532 nm laser beam with the intensity of 100 W cm^{-2} passes through the SnS_2 dispersions, the output intensity of the laser beam is reduced to be 5 W cm^{-2}. This indicates that when a laser beam passes from the reverse (SnS_2/graphdiyne) direction, the intensity of the light beam is severely weakened at the first part of SnS_2 dispersions, after which the laser beam with a reduced intensity continues to pass through the graphdiyne dispersions and cannot excite the diffraction rings. Moreover, the SnS_2 is an RSA material so that the transmittance of the SnS_2 dispersions will decrease when the intensity continues to increase.

The numbers of diffraction rings excited from the independent graphdiyne dispersions and SnS_2 dispersions at λ = 532 nm are shown in Figure 3c. We can find that the diffraction rings of the graphdiyne Ns dispersions can be produced after the laser beam passes through, while the diffraction pattern cannot be excited for the SnS_2 dispersions due to the large bandgap of SnS_2 (2.6 eV). The bandgap of graphdiyne is ≈0.81 eV, which means that the graphdiyne can have a broadband to realize the nonlinear optical response. To summarize: 1) if the laser beam passes from the forward (graphdiyne/SnS_2) direction, the diffraction rings are excited by the first part of graphdiyne dispersions. After that the excited diffraction rings continue to pass through the second part of SnS_2 dispersions, and the ring numbers cannot be changed with the intensity is weakened; 2) If the laser beam passes from the reverse (SnS_2/Graphdiyne) direction, the incident laser beam will be weakened by the first part of SnS_2 dispersions. The weakened laser beam, which has a relatively low intensity below the threshold to excite the diffraction rings of graphdiyne Ns, continues to pass through the second part of graphdiyne dispersion.

Figure 3e,f shows the results of the nonreciprocal light propagation for the proposed graphdiyne/SnS_2-based nonlinear photonic diode at λ = 532 and 671 nm. The result of unidirectional excitation of the diffraction rings can be easily observed. Here the value of N/I is used to represent the strength of NLO response of 2D materials. "N" is the number of diffraction rings and "I" is the intensity of incident laser beam. For comparison, the 532 nm laser beam can have a stronger nonlinear optical response ($N/I \approx 0.11$) than that under the 671 nm laser excitation ($N/I \approx 0.04$). In the SSPM, it is usually the case that an incident light with a lower wavelength can obtain a stronger nonlinear optical response to achieve a larger value of N/I for the 2D materials.[33] Meanwhile, the measured value of N/I reflects the performance of the nonlinear photonic diode. A larger value of N/I indicates that the proposed nonlinear photonic diode can have a more obvious phenomenon of the nonreciprocal light propagation. Therefore, the proposed graphdiyne/SnS_2-based nonlinear photonic diode can have a

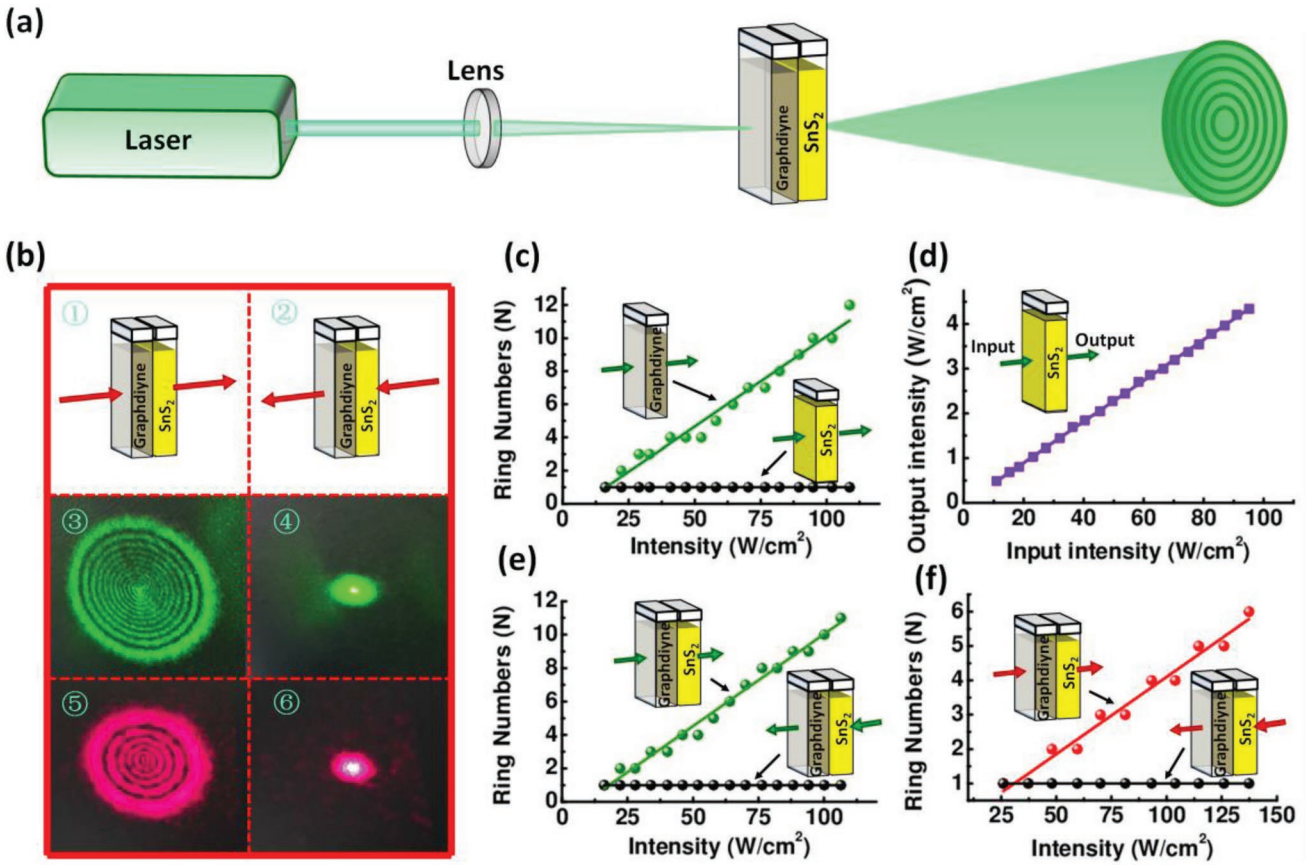

Figure 3. a) The experimental setup for the proposed graphdiyne/SnS_2-based nonlinear photonic diode. b) The phenomenon of the nonreciprocal light propagation observed from the proposed nonlinear photonic diode. c) The number of diffraction rings excited from the independent graphdiyne dispersions and SnS_2 dispersions at $\lambda = 532$ nm. d) The input and output intensity of the 532 nm laser beam before and after it passes through the SnS_2 dispersions. e,f) The results of the nonreciprocal light propagation for the proposed nonlinear photonic diode at $\lambda = 532$ and 671 nm, respectively.

better performance at the wavelength of 532 nm than that at the wavelength of 671 nm. In order to make it closer to real applications, a solid state photonic diode is proposed to realize the nonreciprocal light propagation (**Figure 4**). The dried 2D graphdiyne and SnS_2 were mixed with polymethyl methacrylate (PMMA) to form the graphdiyne-PMMA and SnS_2-PMMA thin films, respectively (Figure 4a), and these two thin films were closely intertwined (Figure 4b,c). After measured, we can also achieve the same phenomenon of the nonreciprocal light propagation from the solid state-based photonic diode (Figure 4d,e).

To further check the performance for the proposed graphdiyne/SnS_2-based nonlinear photonic diode at even lower wavelengths, we studied the proposed photonic diode at $\lambda = 457$ nm (**Figure 5**a). The results show that the diffraction rings can be produced from both the forward (graphdiyne/SnS_2) and reverse (SnS_2/graphdiyne) directions. Although the number of diffraction rings obtain from these two directions are different, the phenomenon of the nonreciprocal light propagation is not as obvious. Therefore, the graphdiyne/SnS_2-based nonlinear photonic diode is not suitable for working at $\lambda = 457$ nm. This might be due to the fact that the 457 nm laser beam (2.71 eV) is beyond the bandgap of SnS_2 (2.6 eV). The appropriate working wavelength for the graphdiyne/SnS_2-based nonlinear photonic diode must be greater than 477 nm (2.6 eV) to ensure the SnS_2 working within its bandgap, which cannot excited the diffraction rings. In our work, we have demonstrated the proposed graphdiyne/SnS_2-based nonlinear photonic diode is suitable to work at the range of 532–671 nm. Figure 5b shows the diffraction rings excited by the independent SnS_2 dispersions at $\lambda = 457$ nm, and the nonreciprocal light propagation of the graphdiyne/SnS_2 hybrid structure at $\lambda = 457$ nm is shown in Figure 5c. The number of diffraction rings produced from the forward (graphdiyne/SnS_2) and reverse (SnS_2/graphdiyne) directions at $\lambda = 457$ nm exists a significant difference, illustrating that the nonlinear refractive indices of these two 2D materials have a large difference.

Here, we proposed a simple and effective similarity comparison method (SCM) to estimate the nonlinear refractive index of the graphdiyne by using the behavior of the nonreciprocal light propagation in photonic diode. The nonlinear refractive index of the graphdiyne can be defined as[30,31]

$$n_2 = \frac{\lambda}{2n_0 L_{\text{eff}}} \cdot \frac{N}{I} \tag{1}$$

where $\lambda / 2n_0 L_{\text{eff}}$ is a known constant, λ, n_0, and L_{eff} are the wavelength of incident laser beam, linear refractive index, and the effective optical thickness of the dispersions. Therefore, if

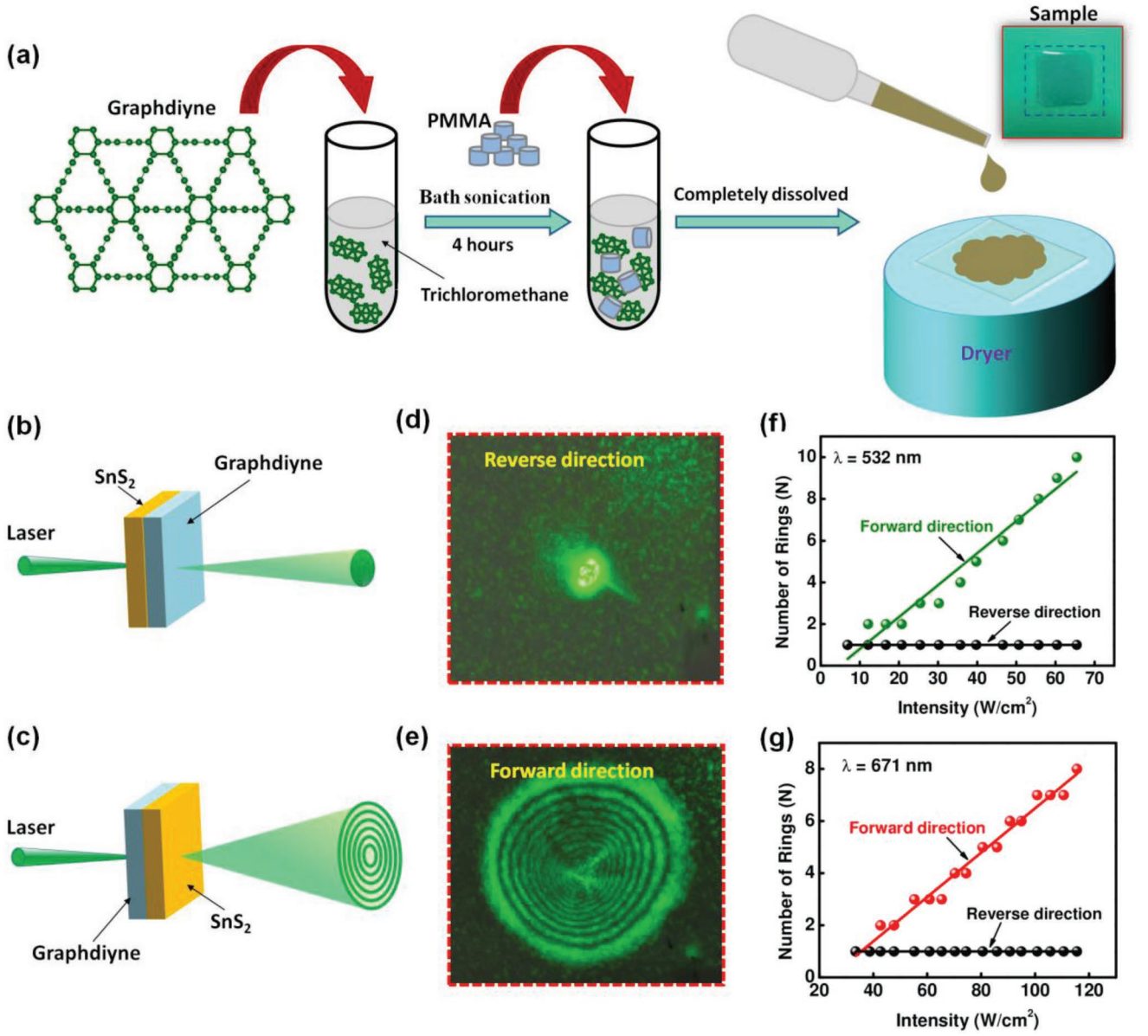

Figure 4. a) Preparation of the graphdiyne-PMMA film. b,c) Experimental setup of the graphdiyne/SnS_2-PMMA film based nonlinear photonic diode. d,e) Images of the diffraction rings obtained from the experiment when the laser beam passes from the forward (graphdiyne/SnS_2) and reverse (SnS_2/graphdiyne) directions of the film-based photonic diode. f,g) The experimental result obtained from the proposed nonlinear photonic diode and the phenomenon of unidirectional diffraction rings excitation can be clearly observed.

the relation of "N" and "I" is measured, the n_2 can be calculated. By comparing the 2D material need to be measured with other materials of known nonlinear refractive indices, we can estimate the nonlinear refractive index of the graphdiyne. The similar contrast (S) can be defined as

$$S = 1 - D = 1 - \frac{|n_{21} - n_{22}|}{n_{21}} = 1 - \frac{\left|\frac{\lambda}{2n_0 L_{\text{eff}}} \cdot \frac{N_1}{I_1} - \frac{\lambda}{2n_0 L_{\text{eff}}} \cdot \frac{N_2}{I_2}\right|}{\frac{\lambda}{2n_0 L_{\text{eff}}} \cdot \frac{N_1}{I_1}} = 1 - \frac{\left|\frac{N_1}{I_1} - \frac{N_2}{I_2}\right|}{\frac{N_1}{I_1}} \quad (2)$$

where D is the difference contrast, n_{21} and n_{22} represent the nonlinear refractive index of the hybrid structure obtained from the forward and reverse directions, respectively. The 2D MoS_2, Bi_2Se_3, SnS, and Sb, whose nonlinear refractive indices are $\approx 10^{-7}$,[52] $\approx 10^{-9}$,[53] $\approx 10^{-5}$,[45] and $\approx 10^{-6}$ cm^2 W^{-1},[54] respectively, are used to compare with graphdiyne (Figure 5d–g). After measurement with SCM, we can obtain the results that the similar contrasts of graphdiyne comparing to SnS_2, Bi_2Se_3, MoS_2, Sb, and SnS are 54%, 58%, 74%, 85%, and 90% (Figure 5h), respectively. This result indicates that the graphdiyne has a similar nonlinear refractive index to those Sb and SnS, which means that the graphdiyne has an n_2 within the range of 10^{-6}–10^{-5} cm^2 W^{-1}. Furthermore, the SnS_2 and Bi_2Se_3

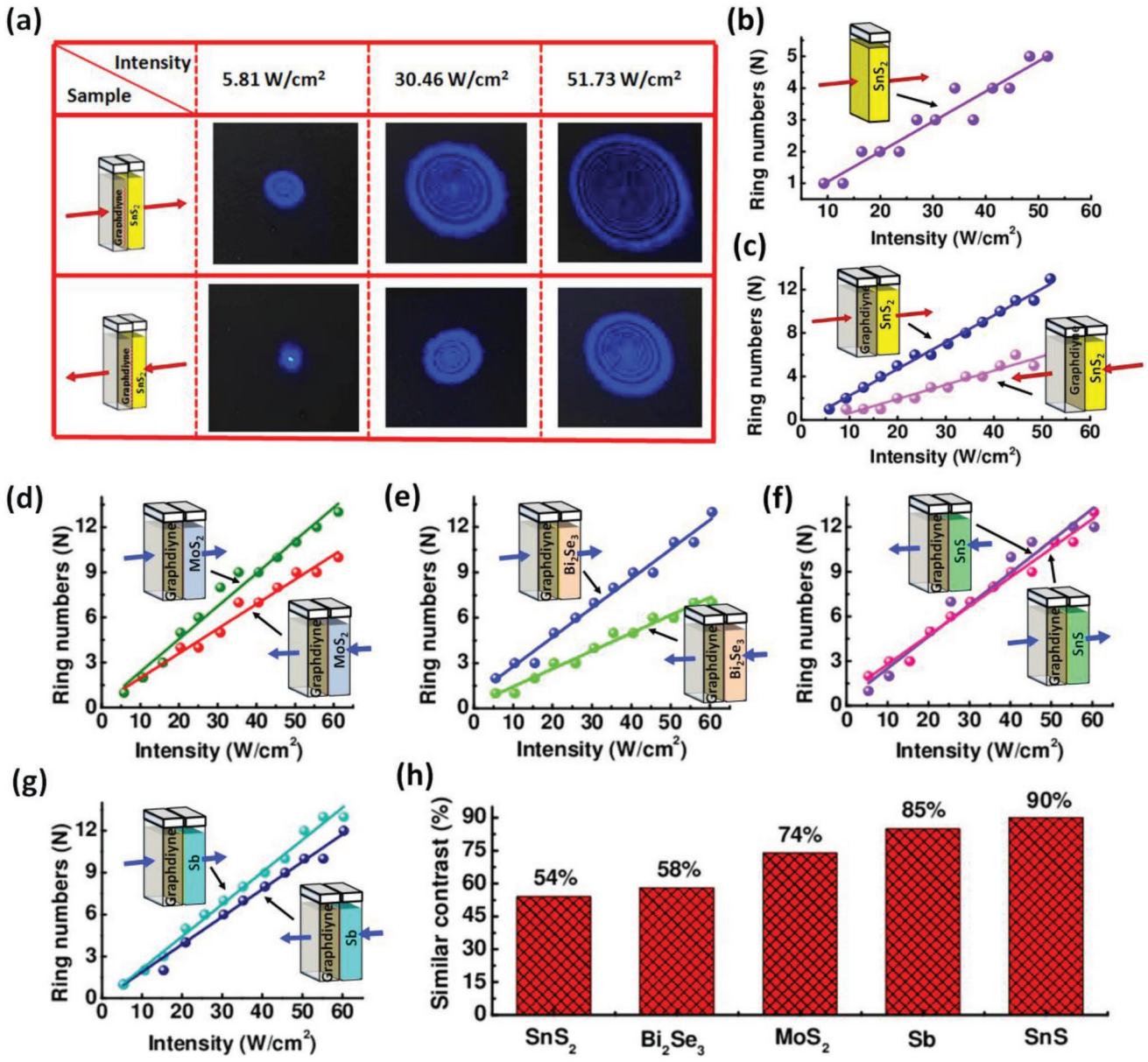

Figure 5. a) The patterns for the phenomenon of the nonreciprocal light propagation obtained at $\lambda = 457$ nm, and the diffraction rings can be observed from the forward (graphdiyne/SnS_2) and reverse (SnS_2/graphdiyne) directions. b) The diffraction rings excited by the independent SnS_2 Ns dispersions at $\lambda = 457$ nm. c) The relation of ring numbers and the intensity of 457 nm laser light. Variation of the diffraction rings with respect to the incident intensity at $\lambda = 457$ nm for the hybrid structures of a) graphdiyne/MoS_2 Ns, b) graphdiyne/Bi_2Se_3 Ns, c) graphdiyne/SnS Ns, and d) graphdiyne/Sb Ns. e) The similar contrast of graphdiyne comparing to other 2D materials (SnS_2, Bi_2Se_3, MoS_2, Sb, and SnS).

have a close value of similar contrast to graphdiyne, illustrating the nonlinear refractive index of SnS_2 is near $\approx 10^{-9}$ cm^2 W^{-1} at $\lambda = 457$ nm.

The mechanism of the interaction between the light and 2D graphdiyne might be summarized in **Figure 6**. As graphdiyne has a direct bandgap of 0.81 eV, the light sources used in our experiment can well interact with the graphdiyne to produce the diffraction rings. When the graphdiyne obtain a photon energy of $E = \hbar\omega$, the electrons in the valence band will be excited into the conduction band, shown in Figure 6a. For SnS_2, the bandgap is as large as 2.6 eV, and the light sources with wavelengths of 671 and 532 nm cannot excite the electrons in SnS_2 from the valence band to the conduction band. This means that the SnS_2 is hard to excite the diffraction rings at $\lambda = 532$ and 671 nm. While the 457 nm laser beam is falling outside the bandgap and can be used to excite the diffraction rings of SnS_2, shown in Figure 6b.

When the laser beams pass from the forward (graphdiyne/SnS_2) direction of the photonic diode, the laser beams will first pass through the part of graphdiyne. In this case, the laser beams (457, 532, and 671 nm) with strong enough intensity can have an interaction with the graphdiyne to excite the

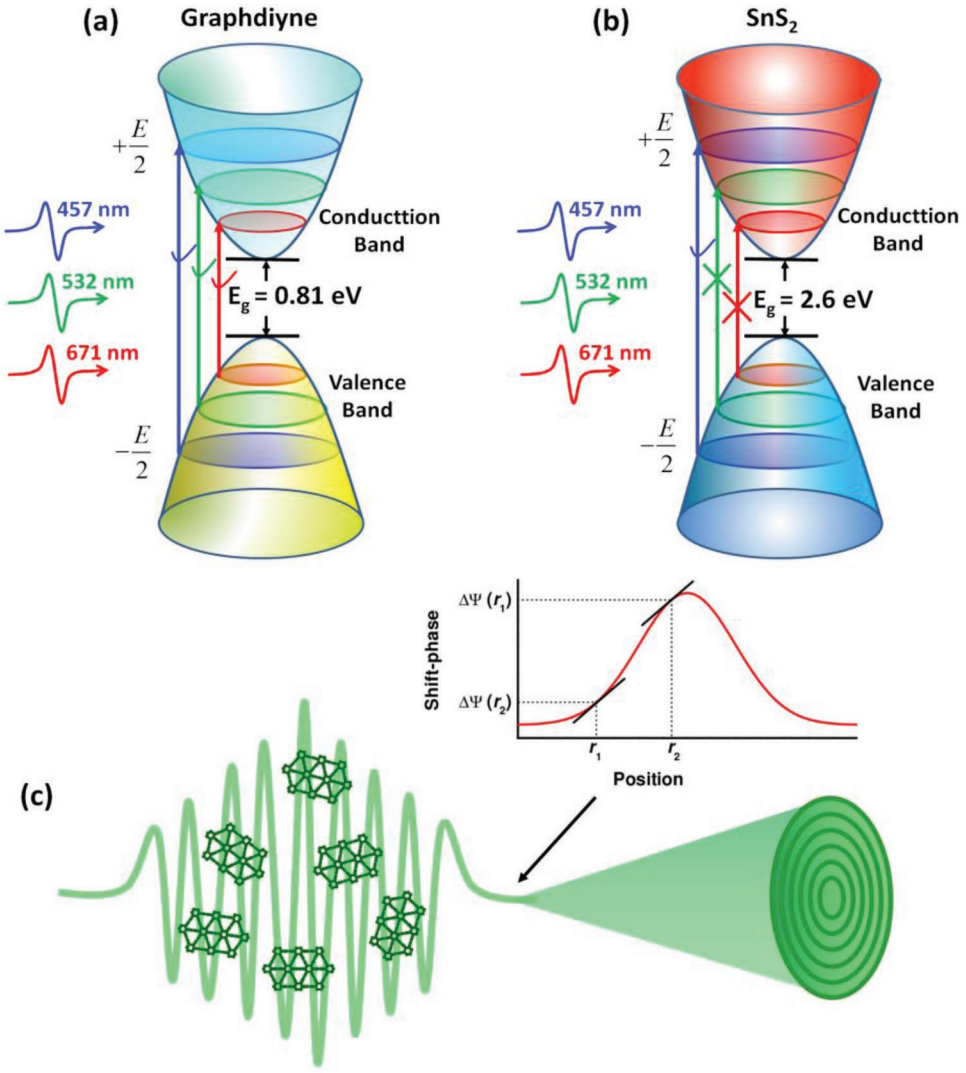

Figure 6. The schematic diagram of the interaction of the incident light with the a) 2D graphdiyne and b) SnS_2. c) The nonlinear optical response manifests itself as diffraction rings for the 2D graphdiyne.

optical Kerr effect and then to produce the diffraction rings due to the narrow bandgap. After the diffraction rings produced at the first part of the graphdiyne, the energy of the laser beams were partially absorbed by graphdiyne and the light diameters were enlarged, so that the light intensity is weakened. Hereafter, the weakened beams (diffraction rings excited by graphdiyne) continue to pass through the second part of the SnS_2, but the diffraction rings of the SnS_2 cannot be excited due to the insufficient intensity and the large bandgap. Finally, we can see the diffraction rings produced from the forward (graphdiyne/SnS_2) direction. Conversely, when the laser beams pass from the reverse (SnS_2/graphdiyne) direction, the laser beam was first pass through the part of SnS_2 with no diffraction rings were excited, and the intensity of the laser beam was greatly weakened due to the RSA behavior of SnS_2. After that, the laser beam continues to pass through the graphdiyne but has not enough intensity to excite the nonlinear diffraction rings for graphdiyne at this time. Finally, we can only see a Gaussian light from the reverse (SnS_2/graphdiyne) direction.

The laser source (457, 532, and 671 nm) used in our experiment is the Gaussian light before interacting with the graphdiyne. After the interaction of the light and graphdiyne, the phase of the light source will have a change due to the Kerr effect. From the curve of phase shift, we can obtain two points of r_1 and r_2 with a same slope: $(\mathrm{d}\Delta\psi/\mathrm{d}r)_{r=r_1} = (\mathrm{d}\Delta\psi/\mathrm{d}r)_{r=r_2}$, which implies that they have the same wave vector to generate interference. The formation process of diffraction rings can be defined as the following equation

$$\Delta\psi(r_1) - \Delta\psi(r_2) = M\pi \quad (M \text{ is an integer}) \tag{3}$$

When M is odd, the dark stripes can be observed in the pattern of diffraction rings. When M is even, the bright stripes can be observed in the pattern of diffraction rings.

In this contribution, nonlinear photonics response of 2D graphdiyne has been revealed by the SSPM method. These results show that graphdiyne possesses a strong nonlinearity to support a broadband NLO response. Taking advantage of

large Kerr nonlinearity in graphdiyne, an interesting configuration of graphdiyne based photonic device has been proposed to realize the unidirectional diffraction rings excitation, and this phenomenon of the nonreciprocal light propagation indicating that the configuration possesses good advance of application in passive photonic diode. In addition, we have proposed a new similarity comparison method to estimate the nonlinear refractive index of graphdiyne and SnS_2. The results show that the graphdiyne has a high similar contrast (≈90%) by comparing to SnS, illustrating that the graphdiyne can have a large nonlinear refractive index (≈10^{-5} cm^2 W^{-1}). Moreover, the SnS_2 is also measured to have a similar nonlinear refractive index with Bi_2Se_3 (≈10^{-9} cm^2 W^{-1}). Our successful application of graphdiyne and SnS_2 in the nonlinear photonic diode allows a universal access of graphdiyne as a new 2D material in a wider range of photonics device applications such as detector, optical information converter, sensors, and switcher.

However, the nonlinear study of graphdiyne is still at an early stage that it needs further investigation of its nonlinear properties or applications in the near future. First, it is demonstrated that the bandgap of graphdiyne can be modulated by doping boron and nitrogen (BN) into the carbon networks of graphdiyne[55] or attaching a homogeneous perpendicular electric field.[56] The NLO response of graphdiyne are closely dependent on its bandgap, and thus it is necessary to further investigate the regulation of the nonlinear response for the graphdiyne by the changed bandgap, and this is the next work that researchers would like to consider. Secondly, graphdiyne possesses a strong Kerr nonlinearity that it is useful to operate as an information converter in all-optical switcher/modulator devices.[33] Thirdly, the saturated absorption behavior of graphdiyne is still not investigated that it may be an interesting work to investigate the saturated absorption of graphdiyne using the method of Z-scan, and further to study the feasibility of the application in light transmittance-based photonic diode.[48] Fourth, graphdiyne shows a strong light-matter interaction with a broadband NLO response that can be coated on the surface of microfiber to develop into an optical Kerr switcher or a four-wave-mixing-based wavelength converter.[57] In a nutshell, 2D graphdiyne exhibits excellent nonlinear properties to possess diverse promising applications in nonlinear photonic devices, such as Kerr switcher, modulator, and wavelength converter.

Experimental Section

Preparation of Graphdiyne/SnS_2-Based Photonic Diode—Solution State-Based Photonic Diode: The prepared graphdiyne dispersions (0.2 mg mL^{-1}) and SnS_2 dispersions (0.25 mg mL^{-1}) were injected into two adjacent cuvettes (5 mm of the thickness), which was the proposed photonic diode. The synthesis of graphdiyne is shown in the Supporting Information.

Preparation of Graphdiyne/SnS_2-Based Photonic Diode—Solid State-Based Photonic Diode: First, 2 mg of the dried graphdiyne was added into 10 mL of the trichloromethane ($CHCl_3$), then sonicated in a water bath for 4 h to ensure that the material was evenly dispersed. After that, the PMMA (3 g) was continuously added into the graphdiyne suspension and stirred for 5 h with a magnetic stirrer. Second, the prepared graphdiyne-PMMA suspension was processed to cover the whole cover glass which placed on a dryer. After half an hour of baking, a sample of graphdiyne-PMMA film with thickness of ≈0.5 mm could be obtained. Third, repeating the previous steps, the graphdiyne-PMMA film could be covered with another layer of SnS_2-PMMA film, and this was the solid state-based photonic diode used in the experiment. Note: Here, PMMA acts as an encapsulation to prevent materials from being contaminated or damaged by direct contact with the surrounding environment.

Experiment Devices: The transmission spectrum from 250 to 1000 nm of graphdiyne is measured by the UV–vis spectrophotometer of UH4150 made by Techcomp. The size distribution of the graphdiyne was obtained in ethanol using a laser particle size analyzer. The crystal features of graphdiyne were characterized by the high-resolution TEM (Tecnai G^2 F30). The material morphology and height were characterized by AFM (Bruker, Dimension Fastscan). In addition, the light sources used in the experiment are 671 nm (MRL-III-671-200 mW), 532 nm (SPROUT-H-5W), and 457 nm (MBL-F-457-400 mW) continuous-wave lasers. The power meter and the charge-coupled device used to receive the light sources are 2936-R and LaserCam-HR II 2/3".

Supporting Information

Supporting Information is available from the Wiley Online Library or from the author.

Acknowledgements

L.W. and Y.D. contributed equally to this work. Financial supports from the Science and Technology Development Fund (Nos. 007/2017/A1 and 132/2017/A3), Macao Special Administration Region (SAR), China, the National Natural Science Foundation of China (NSFC) (61435010, 21773168, 61505117, 11874269, and 61875133), Science and Technology Innovation Commission of Shenzhen (JCYJ20170302153323978 and JCYJ201704101719588539), Tianjin Natural Science Foundation (16JCQNJC05000), and "111 Project" of China (B18030) are acknowledged.

Conflict of Interest

The authors declare no conflict of interest.

Keywords

2D graphdiyne, Kerr nonlinearity, photonic diode, spatial self-phase modulation

Received: December 11, 2018
Revised: January 15, 2019
Published online: February 7, 2019

[1] J. Liu, A. G. Rinzler, H. Dai, J. H. Hafner, R. K. Bradley, P. J. Boul, A. Lu, T. Iverson, K. Shelimov, C. B. Huffman, F. Rodriguez-Macias, Y. S. Shon, T. R. Lee, D. T. Colbert, R. E. Smalley, *Science* **1998**, *280*, 1253.
[2] J. L. Wragg, J. E. Chamberlain, H. W. White, W. Krätschmer, D. R. Huffman, *Nature* **1990**, *348*, 623.
[3] A. F. Hebard, M. J. Rosseinsky, R. C. Haddon, D. W. Murphy, S. H. Glarum, T. T. M. Palstra, A. P. Ramirez, A. R. Kortan. *Nature* **1991**, *350*, 600.
[4] C. Journet, W. K. Maser, P. Bernier, A. Loiseau, M. Lamy de la Chapelle, S. Lefrant, P. Deniard, R. Lee, J. E. Fischer, *Nature* **1997**, *388*, 756.
[5] J. Kong, H. T. Soh, A. M. Cassell, C. F. Quate, H. Dai, *Nature* **1998**, *395*, 878.

[6] K. Hirahara, K. Suenaga, S. Bandow, H. Kato, T. Okazaki, H. Shinohara, S. Iijima, *Phys. Rev. Lett.* **2000**, *85*, 5384.
[7] K. S. Novoselov, A. K. Geim, S. V. Morozov, D. Jiang, M. I. Katsnelson, I. V. Grigorieva, S. V. Dubonos, A. A. Firsov, *Nature* **2005**, *438*, 197.
[8] K. S. Novoselov, A. K. Geim, S. V. Morozov, D. Jiang, Y. Zhang, S. V. Dubonos, I. V. Grigorieva, A. A. Firsov, *Science* **2004**, *306*, 666.
[9] R. R. Nair, P. Blake, A. N. Grigorenko, K. S. Novoselov, T. J. Booth, T. Stauber, N. M. R. Peres, A. K. Geim, *Science* **2008**, *320*, 1308.
[10] G. Li, Y. Li, H. Liu, Y. Guo, Y. Li, D. Zhu, *Chem. Commun.* **2010**, *46*, 3256.
[11] C. Huang, Y. Li, N. Wang, Y. Xue, Z. Zuo, H. Liu, Y. Li, *Chem. Rev.* **2018**, *118*, 7744.
[12] Z. Jia, Y. Li, Z. Zuo, H. Liu, C. Huang, Y. Li, *Acc. Chem. Res.* **2017**, *50*, 2470.
[13] A. Hirsch, *Nat. Mater.* **2010**, *9*, 868.
[14] S. Iijima, T. Ichihashi, *Nature* **1993**, *363*, 603.
[15] J. Chen, J. Xi, D. Wang, Z. Shuai, *J. Phys. Chem. Lett.* **2013**, *4*, 1443.
[16] F. Diederich, Y. Rubin, *Angew. Chem., Int. Ed. Engl.* **1992**, *31*, 1101.
[17] U. H. F. Bunz, Y. Rubin, Y. Tobe, *Chem. Soc. Rev.* **1999**, *28*, 107.
[18] M. Long, L. Tang, D. Wang, Y. Li, Z. Shuai, *ACS Nano* **2011**, *5*, 2593.
[19] G. Van Miert, V. Juričić, C. M. Smith, *Phys. Rev. B* **2014**, *90*, 195414.
[20] Y. Li, L. Xu, H. Liu, Y. Li, *Chem. Soc. Rev.* **2014**, *43*, 2572.
[21] S. Wang, L. X. Yi, J. E. Halpert, X. Y. Lai, Y. Y. Liu, H. B. Cao, R. B. Yu, D. Wang, Y. L. Li, *Small* **2012**, *8*, 265.
[22] H. Qi, P. Yu, Y. Wang, G. Han, H. Liu, Y. Yi, Y. Li, L. Mao, *J. Am. Chem. Soc.* **2015**, *137*, 5260.
[23] K. Srinivasu, S. K. Ghosh, *J. Phys. Chem. C* **2012**, *116*, 5951.
[24] S. L. Zhang, J. J. He, J. Zheng, C. S. Huang, Q. Lv, K. Wang, N. Wang, Z. G. Lan, *J. Mater. Chem. A* **2017**, *5*, 2045.
[25] H. Ren, H. Shao, L. Zhang, D. Guo, Q. Jin, R. Yu, L. Wang, Y. Li, Y. Wang, H. Zhao, D. Wang, *Adv. Energy Mater.* **2015**, *5*, 1500296.
[26] Z. Jin, M. Yuan, H. Li, H. Yang, Q. Zhou, H. Liu, X. Lan, M. Liu, J. Wang, E. dward, H. Sargent, Y. Li, *Adv. Funct. Mater.* **2016**, *26*, 5284.
[27] H. Yan, S. Guo, F. Wu, P. Yu, H. Liu, Y. Li, L. Mao, *Angew. Chem., Int. Ed.* **2018**, *57*, 3922.
[28] V. Nagarajan, U. Srimathi, R. Chandiramouli, *Comput. Theor. Chem.* **2018**, *1123*, 119.
[29] E. Hendry, P. J. Hale, J. Moger, A. K. Savchenko, S. A. Mikhailov, *Phys. Rev. Lett.* **2010**, *105*, 097401.
[30] H. Zhang, S. Virally, Q. Bao, L. K. Ping, S. Massar, N. Godbout, P. Kockaert, *Opt. Lett.* **2012**, *37*, 1856.
[31] S. D. Durbin, S. M. Arakelian, Y. R. Shen, *Opt. Lett.* **1981**, *6*, 411.
[32] R. Wu, Y. Zhang, S. Yan, F. Bian, W. Wang, X. Bai, X. Lu, J. Zhao, E. Wang, *Nano Lett.* **2011**, *11*, 5159.
[33] Y. Wu, Q. Wu, F. Sun, C. Cheng, S. Meng, J. Zhao, *Proc. Natl. Acad. Sci. USA* **2015**, *112*, 11800.
[34] J. Zhang, X. Yu, W. Han, B. Lv, X. Li, S. Xiao, Y. Gao, J. He, *Opt. Lett.* **2016**, *41*, 1704.
[35] B. Shi, L. Miao, Q. Wang, J. Du, P. Tang, J. Liu, C. Zhao, S. Wen, *Appl. Phys. Lett.* **2015**, *107*, 151101.
[36] L. Del Bino, J. M. Silver, M. T. M. Woodley, S. L. Stebbings, X. Zhao, P. Del'Haye, *Optica* **2018**, *5*, 279.
[37] X. Huang, S. Fan, *J. Lightwave Technol.* **2011**, *29*, 2267.
[38] M. Kang, A. Butsch, P. St. J. Russell, *Nat. Photonics* **2011**, *5*, 549.
[39] Z. Shen, Y. L. Zhang, Y. Chen, C. L. Zou, Y. F. Xiao, X. B. Zou, F. W. Sun, G. C. Guo, C. H. Dong, *Nat. Photonics* **2016**, *10*, 657.
[40] K. Fang, J. Luo, A. Metelmann, M. H. Matheny, F. Marquardt, A. A. Clerk, O. Painter, *Nat. Phys.* **2017**, *13*, 465.
[41] K. Gallo, G. Assanto, K. Parameswaran, M. Fejer, *Appl. Phys. Lett.* **2001**, *79*, 314.
[42] L. Feng, M. Ayache, J. Huang, Y. L. Xu, M. H. Lu, Y. F. Chen, Y. Fainman, A. Scherer, *Science* **2011**, *333*, 729.
[43] L. Fan, J. Wang, L. T. Varghese, H. Shen, B. Niu, Y. Xuan, A. M. Weiner, M. Qi, *Science* **2012**, *335*, 447.
[44] Z. Zheng, H. Fang, D. Liu, Z. Tan, X. Gao, W. Hu, H. Peng, L. Tong, W. Hu, J. Zhang, *Adv. Sci.* **2017**, *4*, 1700472.
[45] L. Wu, Z. Xie, L. Lu, J. Zhao, Y. Wang, X. Jiang, Y. Ge, F. Zhang, S. Lu, Z. Guo, J. Liu, Y. Xiang, S. Xu, J. Li, D. Fan, H. Zhang, *Adv. Opt. Mater.* **2018**, *6*, 1700985.
[46] M. Liu, X. Yin, E. Ulin-Avila, B. Geng, T. Zentgraf, L. Ju, F. Wang, X. Zhang, *Nature* **2011**, *474*, 64.
[47] L. Wu, J. Guo, Q. Wang, S. Lu, X. Dai, Y. Xiang, D. Fan, *Sens. Actuators, B* **2017**, *249*, 542.
[48] Y. Dong, S. Chertopalov, K. Maleski, B. Anasori, L. Hu, S. Bhattacharya, A. M. Rao, Y. Gogotsi, V. N. Mochalin, R. Podila, *Adv. Mater.* **2018**, *30*, 1705714.
[49] J. J. Wu, Y. R. Tao, X. C. Wu, Y. Chun, *J. Alloys Compd.* **2017**, *713*, 38.
[50] R. Matsuoka, R. Sakamoto, K. Hoshiko, S. Sasaki, H. Masunaga, K. Nagashio, H. Nishihara, *J. Am. Chem. Soc.* **2017**, *139*, 3145.
[51] J. Zhou, X. Gao, R. Liu, Z. Xie, J. Yang, S. Zhang, G. Zhang, H. Liu, Y. Li, J. Zhang, Z. Liu, *J. Am. Chem. Soc.* **2015**, *137*, 7596.
[52] G. Wang, S. Zhang, X. Zhang, L. Zhang, Y. Cheng, D. Fox, H. Zhang, J. N. Coleman, W. J. Blau, J. Wang, *Photonics Res.* **2015**, *3*, A51.
[53] X. Li, R. Liu, H. Xie, Y. Zhang, B. L. yu, P. Wang, J. Wang, Q. Fan, Y. Ma, S. Tao, S. Xiao, X. Yu, Y. Gao, J. He, *Opt. Express* **2017**, *25*, 18346.
[54] L. Lu, X. Tang, R. Cao, L. Wu, Z. Li, G. Jing, B. Dong, S. Lu, Y. Li, Y. Xiang, J. Li, D. Fan, H. Zhang, *Adv. Opt. Mater.* **2017**, *5*, 1700301.
[55] H. Bu, M. Zhao, H. Zhang, X. Wang, Y. Xi, Z. Wang, *J. Phys. Chem. A* **2012**, *116*, 3934.
[56] Q. Zheng, G. Luo, Q. Liu, R. Quhe, J. Zheng, K. Tang, Z. Gao, S. Nagase, J. Lu, *Nanoscale* **2012**, *4*, 3990.
[57] J. Zheng, Z. Yang, C. Si, Z. Liang, X. Chen, R. Cao, Z. Guo, K. Wang, Y. Zhang, J. Ji, M. Zhang, D. Fan, H. Zhang, *ACS Photonics* **2017**, *4*, 1466.

